



ARC-EN-CIEL beam dynamics

A. Loulergue, M.E. Couprie, C. Bruni

► **To cite this version:**

A. Loulergue, M.E. Couprie, C. Bruni. ARC-EN-CIEL beam dynamics. Particle Accelerator Conference (EPAC08), Jun 2008, Genoa, Italy. pp.115-117. in2p3-00450310

HAL Id: in2p3-00450310

<http://hal.in2p3.fr/in2p3-00450310>

Submitted on 26 Jan 2010

HAL is a multi-disciplinary open access archive for the deposit and dissemination of scientific research documents, whether they are published or not. The documents may come from teaching and research institutions in France or abroad, or from public or private research centers.

L'archive ouverte pluridisciplinaire **HAL**, est destinée au dépôt et à la diffusion de documents scientifiques de niveau recherche, publiés ou non, émanant des établissements d'enseignement et de recherche français ou étrangers, des laboratoires publics ou privés.

ARC-EN-CIEL BEAM DYNAMICS

A. Loulergue, M. E. Couprie, Synchrotron-SOLEIL, Saint-Aubin, France,
C. Bruni, LAL, Orsay France

Abstract

ARC-EN-CIEL project is based on a CW 1.3 GHz superconducting (SC) linac accelerator delivering high charge, subpicosecond and low emittance electron bunches at high repetition rate [1]. According to the electron energy, it provides tunable light sources of high brightness in the VUV to soft X-ray wavelength domain. The project will evolve into three phases: first and second phases are based on high brightness single pass SC linac configuration with a low average current (few μA), while third phase integrates recirculation loops to increase the average current (up to 100 mA).

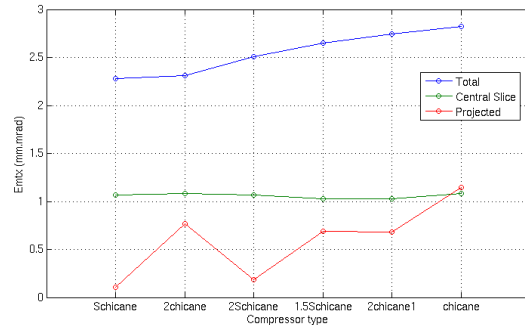


Figure 2: Emittance versus compressors.

INTRODUCTION

This paper focuses on electron beam dynamics issues for the single pass configuration in the two first phases (figure 1) up to one GeV from the RF gun to undulators including magnetic compression stages.

ARC-EN-CIEL INJECTOR

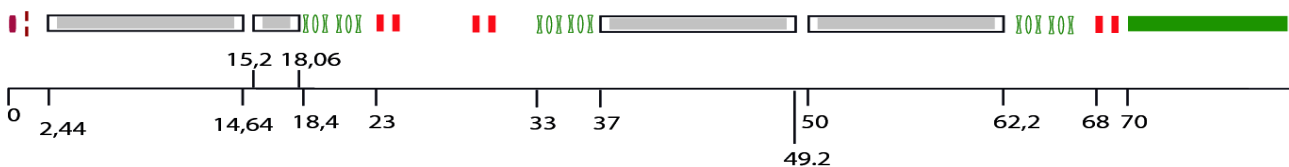
The layout for ARC-EN-CIEL high peak brightness is based on the FLASH [2] injector composed of an RF gun photo-injector [3], one RF cryomodule followed by a third harmonic cavity linearizer and finally by the magnetic compressor. With a maximum gun voltage of 40 MV/m the energy reaches about 4 MeV at the exit of the gun. The cryomodule is composed of 8 cavities with a mean gradient of 14 MV/m increasing the energy up to a maximum of 120 MeV. A configuration with a compensating [4] coils (max field of 0.171 T) located at 24 cm from the cathode, gives a minimum total emittance

of the order of $1.1 \pi \cdot \text{mm} \cdot \text{mrad}$ at the exit of the first modules [5]. The laser pulse duration is 20 ps beer-can-like uniform distributions with 2 ps rise and fall times at both edges and the total bunch charge is 1 nC. The laser spot radius on the cathode is set to 1.7 mm giving a $0.7 \pi \cdot \text{mm} \cdot \text{mrad}$ of thermal emittance. Simulations are performed using Astra code [6].

ARC-EN-CIEL COMPRESSOR

We test different variations of magnetic compressors located just after the injector based on simple sets of dipoles (chicane, double chicane, S-chicane, etc ..). In order to compare their effects on emittance degradation (CSRtrack code [7]), we impose to all of them the same overall length of 10 m, the same compression factor of $r_{56}=0.2$ m and the same optics (i.e. a strong converging beta function from 100 to 2 m). In all cases the bunch is compressed from 2 mm to 0.140 mm rms length keeping the same output current profile as plotted in figure 3.

ARC-EN-CIEL Phase 1



ARC-EN-CIEL Phase 2

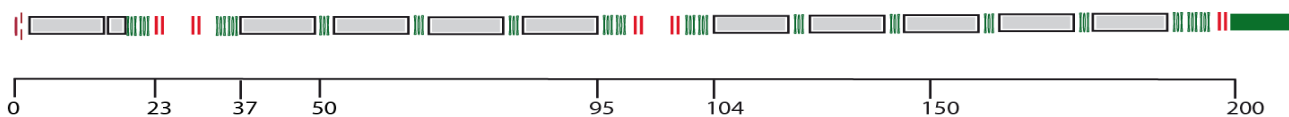


Figure 1 : Layouts of ARC EN CIEL phase 1 (330 MeV) and 2 (1 GeV).

The different emittance increases are plotted in figure 2 sorted in ascending order with respect to the total emittance. The best solutions are given by either S-chicane or double-reversed chicane with a total emittance increase from 1 to $2.3 \pi \cdot \text{mm} \cdot \text{mrad}$. They are very similar and the S-chicane could be simply assimilated to a double chicane without the central magnets. The worst compressor is the simple chicane with a total emittance increase from 1 of $2.8 \pi \cdot \text{mm} \cdot \text{mrad}$. It can be simply explained by the presence of higher magnetic field especially in the last dipole where the emittance increase happens. In between there are other chicane variations, such as double chicane, 1.5-Schicane and 2S-chicane. In every case there are no slice emittance increases and the projected emittance tends to be lower for the S-chicane compressor. The total emittance increase is mainly due to strong mismatch between slices and the projected emittance.

ARC-EN-CIEL PHASE 1 & 2

Phase 1 and 2 present the main linac with a final energy of 330 MeV and 1 GeV respectively (figure 2). They include an RF gun photo-injector with a maximum voltage of 40 MV/m, a set of TESLA RF cryomodules with a mean gradient of 14 MV/m, a third harmonic cavity linearizer and magnetic compressors.

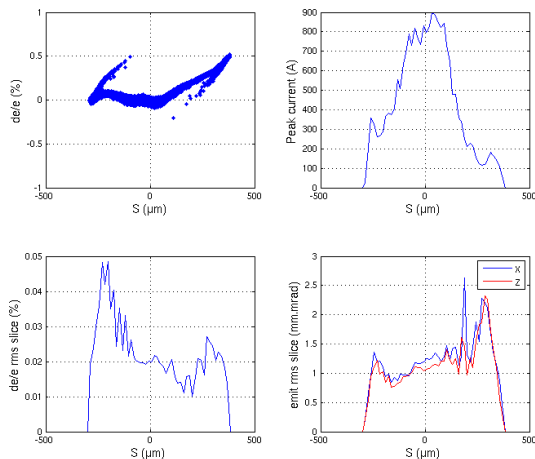


Figure 3 : Phase 1 longitudinal phase space, peak current, slice emittances and energy spread at 220 MeV.

In phase 1, a 10 m S-chicane magnetic compressor located down stream of the first TESLA cryomodule and the third harmonic cavity allows to compress the bunch from 2 mm down to $140 \mu\text{m}$ rms at an energy of about 100 MeV with a compression factor of $r_{56}=0.2$ m. The slice emittances are preserved while the projected one is increased to $0.1 \pi \cdot \text{mm} \cdot \text{mrad}$. The total emittance is then increased to $2.3 \pi \cdot \text{mm} \cdot \text{mrad}$ mainly due to strong mismatch between the slices and the projected phase space alignment. The current profile exhibits a flat top of 550 fs ($150 \mu\text{m}$) at a

peak current of 800 A with an energy spread of 1 to $2 \cdot 10^{-4}$. Two other TESLA RF cryomodules are added to reach a maximum final energy of 330 MeV. At this maximum energy, there is a remaining energy chirp of few 10^{-4} in the central region. It can be canceled by strong off-crest phasing (60°) of two downstream Tesla RF cryomodules. The final energy is then reduced to 220 MeV (figure 3).

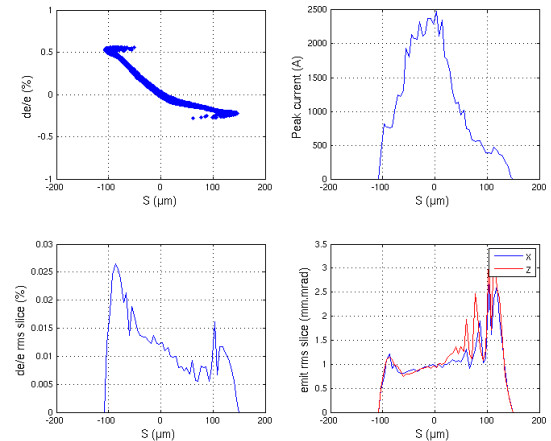


Figure 4 : Phase 2 longitudinal phase space, peak current, slice emittances and energy spread at 1 GeV.

In phase 2, 7 other TESLA cryomodules are added raising the final energy up to 1 GeV. The first compressor is kept at an energy of 100 MeV and a second one is added at mid energy around 500 MeV downstream of the next 4 cryomodules, the remaining 5 cryomodules end the linac. The bunch is then compressed from 2 mm down to $320 \mu\text{m}$ rms in the first 10 m S-chicane stage without any emittance deterioration with a compression factor of $r_{56}=0.1$ m. In the second identical S-chicane compressor, the bunch length is further compressed down to $50 \mu\text{m}$ rms with a lower compression factor of $r_{56}=0.05$ m. Here again, the slice emittances are preserved while the projected one is increased to $0.14 \pi \cdot \text{mm} \cdot \text{mrad}$. The total emittance is then increased to $1.6 \pi \cdot \text{mm} \cdot \text{mrad}$. The current profile exhibits a flat top of 200 fs ($60 \mu\text{m}$) at a peak current of 2000 A with an energy spread of 10^{-4} (figure 4). Here again, at this maximum energy of 1 GeV, there is a remaining energy chirp of few 10^{-4} in the central region.

OPTIMISATION OF THE BUNCH BRIGHTNESS

Further investigations have been undertaken on bunch brightness optimization including a compression stage. They are based on the lengthening of the laser pulse duration from 20 to 40 ps as well as raising the gun voltage from 40 to 60 MV/m to reduce the thermal emittance component by means of spot size reduction on the cathode. Besides these thermal component reductions, the effect of the space charge distortions are also reduced

by a higher acceleration or by the linearizing of the transverse space charge effect for longer cylindrical bunches where distortions are pushed toward the edges. Further laser duration lengthening have been also investigated, but combination of RF and space charge distortion combined with a higher compression rate make the compression more difficult to control.

With 20 ps and 40 MV/m, the slice emittances are about 1π .mm.mrad, they are reduce down to 0.6 by lengthening the laser pulse to 40 ps and furthermore reduced to 0.4 by increasing the voltage to 60 MV/m. In this later case, they are equal to the thermal component contribution. The total emittance is more or less unchanged by lengthening the laser pulse from 20 to 40 ps. It is more difficult to get a good compensation with longer pulse. It is reduced from 1 to 0.8 π .mm.mrad by increasing the voltage from 40 to 60 MV/m.

The use of the an ellipsoidal laser [8] pulse shape that has the advantage to cancel space charge distortion has also been envisaged. Without space charge distortion, it is possible to increase the electron density on the cathode close to cancel the accelerating field. Simulations exhibit

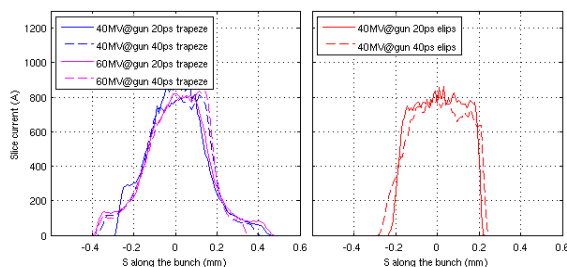


Figure 5: Current profile after compression to 800 A.

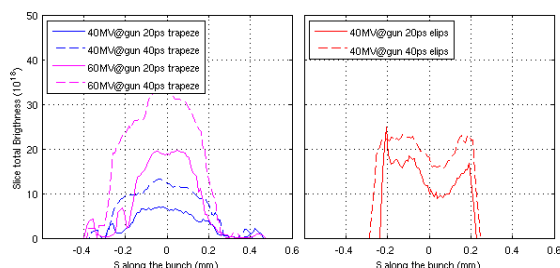


Figure 6: Slice total brightness after compression.

a possible reduction by 20 % of the central slice thermal emittance for 20 ps laser pulse. For longer laser pulse, this reduction is less and less effective. The slice emittance follows the same parabolic profiles than the current. The total emittance is then smaller than the central slice and also smaller than the trapezoidal case. Another advantage of this distribution is to, in principle, cancel the slice-to-slice space charge mismatch. The downstream re-matching process is then easier and less sensitive.

After compression, for trapezoidal cases, lengthening the laser pulse from 20 to 40 ps allows to increase the brightness by about a factor 2. Increasing the gun voltage

from 40 to 60 MV/m allows a higher increase by a factor of almost 3. The brightness profile is close to the current profile with a flat top of about 600 fs. From the standard ARC-EN-CIEL case (40 MV/m, 20 ps) to 60MV/m, 40 ps, a factor of about 6 is obtained on the brightness.

For the two ellipsoidal cases, the total brightness exhibits a curved shape along the slices with a minimum in the central region. It directly comes from the flat-topped current together with smaller emittances on each side. With 40 MV/m and 20 ps, the ellipsoidal distribution allows us to gain a factor from 2 to 3 in the brightness. As expected, for longer pulse durations this gain is less effective. With 40 ps, it is only a factor from 1.5 to 2.

Investigating longer pulse, it is naturally interesting to investigate also the possible velocity bunching in the early stage of the acceleration as a complement [9]. We use the same set up as that simulated at FLASH [10]. The phase of the first cavity of the RF cryomodule is tuned off-crest giving a strong energy chirp. The head particles are decelerated but, unfortunately, the tail particles are not accelerated due to the fact that at 4 MeV (RF gun exit energy), they are already close to the light velocity. As a consequence, it is possible to compress the bunch but with strong longitudinal distortions with respect to the bunch center. It is then very difficult to further increase the peak current by mean of magnetic compressors, where linear phase space chirps are required. Nevertheless, a smaller total emittance is possible with a small compression ($\sim 10\%$). In the case 40 ps and 40 MV, the total emittance is reduced from 1.1 to 0.7 π mm.mrad.

ACKNOWLEDGEMENT

This work has been supported by the EU commission in the sixth framework program, contract 011935 – EUROFEL.

REFERENCES

- [1] M.E. Couprie et al., <http://arcenciel.synchrotron.fr/ArcEnCiel>
- [2] J. Rossbach, 'A VUV free electron laser at the TESLA test facility at DESY', NIM sec. A, vol. 375, 1996.
- [3] S. Scheiber et al., The injector of the VUV-FEL at DESY, Proceeding FEL 2005.
- [4] B. E. Carlsten, New Photoelectric Injector Design for the Los Alamos National Laboratory XUV FEL Accelerator, Nucl. Instr. Meth. A 285, (1989), 313.
- [5] P. Piot, Private communication.
- [6] K. Floettman, ASTRA code, <https://www.desy.de/mpyflo/>
- [7] M. Dohlus and T. Limberg, "CSRtrack", <http://www.desy.de/xfel-beam/csrtrack/index.html>
- [8] C. Limberg and P. Bolton, Optimum electron distributions for space charge dominated beams in photoinjectors, Nucl. Instr. Meth. A 557, (2006), 106.
- [9] L. Serafini, M. Ferrario, Velocity Bunching in Photo-Injector, AIP, 2001.
- [10] B. Beutner et al., Velocity Bunching at XFEL, PAC, 2007.